~~RESTRICTED~~

RM No. A7B06

RESEARCH MEMORANDUM

THE CALCULATION OF DRAG FOR AIRFOIL SECTIONS AND BODIES OF REVOLUTION AT SUBCRITICAL SPEEDS

By

Max. A. Heaslet and Gerald E. Nitzberg

Ames Aeronautical Laboratory
Moffett Field, Calif.

~~This document contains classified information affecting the National Defense of the United States within the meaning of the Espionage Act, USC 50:31 and 32. Its transmission or the revelation of its contents in any manner to an unauthorized person is prohibited by law.~~
~~Information so classified may be imparted only to persons in the military and naval services of the United States, appropriate civilian officers and employees of the Federal Government who have a legitimate interest therein and to United States citizens of known loyalty and discretion who of necessity must be informed thereof.~~

NATIONAL ADVISORY COMMITTEE
FOR AERONAUTICS

WASHINGTON

April 23, 1947

~~RESTRICTED~~

FILE

National Aeronautics and
Space Administration

Langley Research Center
Hampton, Virginia
23665

NASA

Reply to Attn of 139A

JUN 16 1983

TO: Distribution

FROM: 180A/Security Classification Officer

SUBJECT: Authority to Declassify NACA/NASA Documents Dated Prior to January 1, 1960

Effective this date, all material (informal, correspondence) classified by this Center prior to January 1, 1960, is declassified. This action does not include material derivatively classified at the Center upon instructions from other Agencies.

Immediate re-marking is not required; however, until material is re-marked by lining through the classification and annotating with the following statement, it must continue to be protected as if classified:

> "Declassified by authority of LaRC Security Classification Officer (SCO) letter dated June 16, 1983," and the signature of person performing the re-marking.

If re-marking a large amount of material is desirable, but unduly burdensome, custodians may follow the instructions contained in NHB 1640.4, subpart F, section 1203.604, paragraph (h).

This declassification action complements earlier actions by the National Archives and Records Service (NARS) and by the NASA Security Classification Officer (SCO). In Declassification Review Program #07008, NARS declassified the Center's "Research Authorization" files, which contain reports, Research Authorizations, correspondence, photographs, and other documentation. Earlier, in a 1971 letter, the NASA SCO declassified all NACA/NASA formal series documents with the exception of the following reports, which must remain classified:

Document No.	First Author
E-51A30	Nagey
E-53G20	Francisco
E-53G21	Johnson
E-53K18	Spooner
SL-54J21a	Westphal
E-55C16	Fox
E-56H23a	Himmel

JUN 23 1983

If you have any questions concerning this matter, please call Mr. William L. Simkins at extension 3281.

Jess G. Ross
2898

Distribution:
SDL 031

cc:
NASA Scientific and Technical
Information Facility
P.O. Box 8757
BWI Airport, MD 21240

NASA--NIS-5/Security
180A/RIAD
139A/TU&AO
139A/WLSimkins:elf 06/15/83 (3281)
139A/JS 6-15-83

31-01 HEADS OF ORGANIZATIONS
HESS, JANE S.,
MAIL STOP 168 BLDG 1194

NATIONAL ADVISORY COMMITTEE FOR AERONAUTICS

RESEARCH MEMORANDUM

THE CALCULATION OF DRAG FOR AIRFOIL SECTIONS AND BODIES OF REVOLUTION AT SUBCRITICAL SPEEDS

By Max. A. Heaslet and Gerald E. Nitzberg

SUMMARY

A method is developed for calculating the drag, in a real compressible fluid and at subcritical Mach numbers, of airfoil sections at arbitrary lift coefficients and of bodies of revolution at zero angle of attack. To apply the method it is necessary to know the velocity distribution for airfoils and the velocity and thickness distributions for bodies of revolution, together with the Mach number of the free-stream transition point from laminar to turbulent flow, and the Reynolds number based on chord or axial length. The method consists of tracing the growth of momentum thickness along the surface, for both the laminar and turbulent boundary layers, by means of relations which involve elementary integrals and can be evaluated by simple numerical means. An outline of the computational procedures required for drag calculations is presented in the appendix to the report.

The values of drag coefficient, computed by the method of the present report for a number of cases, are compared with the values obtained for the same configurations by other methods and the differences between the various results are found to lie within the limits of accuracy of current experimental techniques. The use of the present method is recommended by its simplicity and generality.

INTRODUCTION

Starting with the work of Prandtl (reference 1), which was designed to determine the skin friction on a pointed flat plate in a uniform incompressible two-dimensional flow, the theory of drag calculations has been extended by several investigators so that, under controlled conditions and at speeds where air may be assumed an incompressible medium, very good agreement has been obtained with experiment for both airfoil sections and streamlined bodies of revolution. The calculation of drag is, however, limited to cases for which it is possible to estimate the location of the transition point, that is, the point at which the laminar boundary layer over the forward portion of the body is terminated by the

onset of turbulent flow, and for which there is no extensive separation of the turbulent boundary layer.

In the present report the compressibility of the medium is considered and expressions for profile drag of airfoil sections and bodies of revolution at subcritical Mach numbers are given in forms which are particularly amenable to numerical calculation. The principal contribution, however, is contained in the treatment of the turbulent boundary layer in the two cases. As in previous work on this subject, the solutions consist essentially of integrals of the Kármán moment equation for bodies in two-dimensional flow and for flow over three-dimensional bodies with axial symmetry. In reference 2, Squire and Young solve the problem for incompressible flow in two dimensions by means of a point-by-point method of integration requiring considerable labor, and in references 3, 4, 5, and 6 modifications of the Squire and Young method are given in various forms which expedite the calculations. All these references give results which are in close agreement. The method of Kalikhman in reference 6 is of particular interest for it is capable of generalization to the body of revolution and to the case of high-speed flow where density changes are of sufficient magnitude that they must be taken into account. This approach is adopted in the present report.

The various procedures which have been developed for predicting the growth of the turbulent boundary layer over an airfoil are all based on the same boundary-layer momentum equation. In order to apply this equation it is necessary first to relate the skin-friction coefficient to the boundary-layer momentum thickness. On the basis of experimental data for flat plates two such relationships have been evaluated: a power law (reference 7) and a logarithmic law (references 8 and 2). After comparison with the experimental data shown by Falkner in reference 7, for Reynolds numbers between 2×10^6 and 5×10^7, it appears that there is little significant difference in the numerical values of these two relations, when the scatter of the experimental data is taken into consideration. The logarithmic law can be generalized easily to the case of compressible flow and is used in the analysis of this report.

The logarithmic relationship between the skin-friction coefficient and the boundary-layer momentum thickness was combined by Squire and Young with the boundary-layer momentum equation to obtain the section drag of airfoils. The step-by-step integration of the fundamental equation was first avoided in reference 4 where it was found that a considerable simplification can be achieved by dividing the velocity distribution over the airfoil into segments in each of which the chordwise velocity gradient is relatively constant. Then, using an average value of the velocity gradient for each segment, it was found possible to construct a general graph from which the solution for any velocity distribution can be read. The authors of the present report were able to generalize the method

of reference 4 to the case of compressible flow over airfoil sections but the results have never been published. It was thought that the closed form in which the present results are given, together with the duality which it was possible to establish between the two- and three-dimensional cases, make the latter approach preferable.

The power law relationship postulated by Falkner has been used in reference 3 by Holt to obtain a directly integrable relation for the turbulent boundary-layer growth. By means of a theoretical approach based on experimental results Tetervin (reference 5) related the skin-friction coefficient and boundary-layer momentum thickness in a more complex form which varied with the boundary-layer Reynolds number. Approximating this expression, over the range of integration, by a power law, Tetervin was able to express the growth of the turbulent layer in a manner somewhat analogous to that of Holt. The final forms resulting from this method of approach share with the present results for the turbulent layer the advantage of being in closed form. In reference 9 Tetervin has extended his method to include both two- and three-dimensional compressible flow.

In the vicinity of the airfoil leading edge there is always a more or less extensive region of laminar boundary-layer flow. For airfoils at flight Reynolds numbers the laminar portion of the boundary layer contributes a minor portion of the total section drag; however, the amount is usually not negligible. In reference 10, Young and Winterbottom present a method for laminar boundary-layer calculations which includes compressibility effects. The derivation of their method is comparable to that of reference 11. There are, however, two significant differences: First, reference 10 is based on Pohlhausen's relationship for the velocity variation through the boundary layer, while reference 11 uses the Blasius velocity profile; and, second, reference 10 neglects the fact that for air Prandtl's number is not equal to unity. The method of reference 11 is used in the present report.

Most of the theoretical and experimental work on bodies of revolution to date has been on airship shapes. With the present trend, however, toward large land-based airplanes, particularly those with pressurized cabins, it is to be expected that fuselage shapes will approach bodies of revolution. The problem of studying the boundary-layer growth and the drag of bodies of revolution thus takes on increased significance while at the same time it becomes necessary to generalize the procedure to include the effects of compressibility. The development of the laminary boundary layer over bodies of revolution in a compressible fluid is given in reference 11 and the theory given there is applied directly in the present report. The momentum equation of the turbulent boundary layer is given by Young in reference 12 for zero angles of incidence and a step-by-step method of integration is presented whereby the growth of the boundary layer may be determined for incompressible

flow. The boundary-layer equations, for both turbulent and laminar flow, are more complicated for the body of revolution than for an airfoil section because of the fact that is is necessary to take into consideration the variation of the body radius along the axis.

Drag calculations for bodies of revolution have not been studied as extensively as for airfoils and little previous work in the field of compressible flow has as yet been published. The present theory is similar to that developed for airfoil sections in that momentum loss in the boundary layer is expressed as a definite integral but differs in that it becomes necessary to modify the theory over the far aft portion of the body. In spite of this difficulty the method given does curtail sharply the amount of time required for the total calculation.

A complete list of symbols, as used throughout this report, may be found in Appendix A, and the computational procedure for drag calculations is presented in Appendix B.

THEORY

Airfoil Sections

Introductory remarks.- In figure 1 the two-dimensional flow about an airfoil section is indicated along with the boundary layer and wake associated with the flow. It is an established practice, in all theory connected with the calculation of drag, to divide the boundary layer and wake region into three different regimes of flow. Thus, if S represents the stagnation point, the boundary layer between S and the transition point at T.P. on either surface is laminar while between T.P. and the trailing edge at T.E. a turbulent boundary layer exists. In the wake, the third region to be considered, the plane AA is drawn normal to the center line of the wake at the point where static pressure in the wake has returned to its original free-stream value.

It is easy to show, from momentum considerations, that if static pressure is assumed constant across the wake, then the drag D per unit length of the airfoil is given by

$$D = \int_w \rho u(U_o - u)dy \qquad (1)$$

where the integration extends across the wake in plane AA and

u local velocity in wake

ρ density in wake

U_o velocity of undisturbed stream

y distance measured normal to center line of wake

Momentum thickness of the boundary layer is, by definition,

$$\theta = \int_0^{\delta} \frac{\rho u}{\rho_U U}\left(1 - \frac{u}{U}\right) dy \tag{2}$$

where

U velocity at edge of boundary layer

u local velocity in boundary layer

y distance measured normal to surface

θ momentum thickness of boundary layer

δ boundary-layer thickness

ρ_U density corresponding to velocity U

and in a similar manner the momentum thickness of the wake may be defined. Now let

$$\theta_2 = \int_w \frac{\rho u}{\rho_o U_o}\left(1 - \frac{u}{U_o}\right) dy \tag{3}$$

where the integration is in plane AA and ρ_o is density corresponding to free-stream velocity U_o. Since drag coefficient c_d is fixed by the relation

$$D = c_d \frac{1}{2} \rho_o U_o^2 c \tag{4}$$

where c is the chord length of the airfoil, it follows that

$$c_d = \frac{2\theta_2}{c} \tag{5}$$

The analysis consists essentially in tracing the growth of θ, the momentum thickness, along the top and bottom surface of the airfoil and in the wake to the plane AA. Since the nature of the flow in the boundary layer affects the rate of growth of the momentum thickness, it is necessary to treat the different regimes separately. The following development is therefore arranged to conform with this natural division.

Laminar layer.- In reference 11, expressions have been developed which may be applied immediately to determine the growth of the laminar boundary layer in two-dimensional flow of a compressible

fluid. In this reference the boundary-layer thickness d_1 at the point x_1 is defined as the distance from the surface of the airfoil to a point in the boundary layer where the ratio of the local velocity to the velocity outside the boundary layer is 0.707. Neglecting terms involving the fourth power of M, where M is the Mach number of the free stream, the boundary-layer thickness d_1 is given by the relation

$$\left(\frac{d_1}{c}\right)^2 = \frac{1}{R_c\left(\frac{U_1}{U_o}\right)^{9.17}}\left[5.3\left\{1-0.35M^2\left[1-1.91\left(\frac{U_1}{U_o}\right)^2\right]\right\}\right.$$

$$\left.\int_o^{\left(\frac{x}{c}\right)_1}\left(\frac{U}{U_o}\right)^{8.17}d\left(\frac{x}{c}\right)-0.44\,M^2\int_o^{\left(\frac{x}{c}\right)_1}\left(\frac{U}{U_o}\right)^{10.17}d\left(\frac{x}{c}\right)\right] \qquad (6a)$$

where

R_c Reynolds number based on chord length

U_1 velocity outside boundary layer at point x_1

U velocity outside boundary layer at point x

x distance along airfoil chord

In the computation of section drag coefficients, inasmuch as the laminar portion of the boundary layer contributes a minor portion of the total drag, it is practicable to simplify this equation. The modification will concern itself with the last term in equation (6a) and is justified by the fact that the last term contributes a small part to the total value of the boundary-layer thickness squared. Approximating the last term by the expression

$$-\frac{5.3\,M^2}{\left(\frac{U_1}{U_o}\right)^{9.17}R_c}\left(\frac{U_1}{U_o}\right)^2(0.083)\int_o^{\left(\frac{x}{c}\right)_1}\left(\frac{U}{U_o}\right)^{8.17}d\left(\frac{x}{c}\right)$$

equation (6a) may be rewritten as

$$\left(\frac{d_1}{c}\right)^2 = \frac{5.3}{R_c\left(\frac{U_1}{U_o}\right)^{9.17}}\left\{1-0.35M^2\left[1-1.67\left(\frac{U_1}{U_o}\right)^2\right]\right\}$$

$$\int_o^{\left(\frac{x}{c}\right)_1}\left(\frac{U}{U_o}\right)^{8.17}d\left(\frac{x}{c}\right) \qquad (6b)$$

Again neglecting terms involving the fourth power of M, it is possible to show from results given in the reference that if Prandtl's number $Pr = \frac{c_p \mu}{k}$ is set equal to 0.733, its value for free air, then

$$\left(\frac{\delta}{d}\frac{\rho U}{\rho_o}\right)_1^2 = 0.082\left\{1 + 0.61\,M^2\left[1 - 1.34\left(\frac{U_1}{U_o}\right)^2\right]\right\} \tag{7}$$

In the calculations that follow the basic variable will be the nondimensional product of momentum thickness and density. The value of this variable at the point $x = x_1$, independent of the definition of boundary-layer thickness, is an immediate consequence of equations (6b) and (7). Thus

$$\left(\frac{\theta}{c}\frac{\rho U}{\rho_o}\right)_1^2 = \frac{0.43}{R_c\left(\frac{U_1}{U_o}\right)^{8.17}}\left\{1 + 0.26\,M^2\left[1 - 0.92\left(\frac{U_1}{U_c}\right)^2\right]\right\} \int_0^{\left(\frac{x}{c}\right)_1}\left(\frac{U}{U_o}\right)^{8.17} d(x/c) \tag{8}$$

Turbulent layer.- The momentum equation for the turbulent boundary layer in compressible flow is given in reference 10 as

$$\frac{d\theta}{dx} + \left[(H + 2)\frac{U'}{U} + \frac{\rho_U'}{\rho_U}\right]\theta = \frac{\tau}{\rho_U U^2} \tag{9}$$

where the primes indicate differentiation with respect to x, H is a function of the boundary-layer velocity-profile shape, and τ is the skin friction per unit area. Under the assumption that, for compressible fluids,

$$\frac{U\rho_U\theta}{\mu_w} = 0.2454\,e^{0.8814\zeta} \tag{10}$$

where

$$\zeta^2 = \frac{\rho_U U^2}{\tau}$$

and μ_w is the coefficient of viscosity at the wall, it is

possible to transform the equation to the form used by Young and Winterbottom

$$\frac{d\zeta}{dx} + 2.555\ (H + 1)\frac{U'}{U} = \frac{U\rho U}{\mu_w}\ 10.411\zeta^{-2}e^{-0.3914\zeta} \qquad (11)$$

The numerical methods used in the integration of equation (11) are somewhat protracted. To obviate this introduce now the transformation

$$z = \frac{U\theta\rho U}{\mu_w}\ \zeta^2 = 0.2454\zeta^2\ e^{0.3914\zeta} \qquad (12)$$

With this change of variable, equation (11) becomes

$$\frac{dz}{d\left(\frac{x}{c}\right)} + K\ (H+1)\frac{\left[d(U/U_o)/d(x/c)\right]}{U/U_o}\ z = K\ \frac{U}{U_o}\ \frac{U_o\rho_o c}{\mu_w}\ \frac{\rho U}{\rho_o} \qquad (13)$$

where

$$K = 2.555\left(0.3914 + \frac{2}{\zeta}\right)$$

and the equation has been written in nondimensional form.

It is necessary in equation (13) to relate the value of coefficient of viscosity at the wall to its value in the free stream μ_o. This follows directly from the empirical relation (reference 13)

$$\frac{\mu_o}{\mu_w} = \left(\frac{T_o}{T_w}\right)^{0.76}$$

where T_o and T_w are absolute temperatures in the stream and at the wall, together with

$$T_w = T_o\left(1 + \frac{\gamma-1}{2}\ M^2\right)$$

which is an immediate consequence of the assumption that energy is constant through the turbulent boundary layer. It follows that, approximately,

$$\mu_w = \mu_o\ (1 + 0.152\ M^2) \qquad (14)$$

Setting

$$\frac{U}{U_o} = \overline{U}, \quad \frac{\rho U}{\rho_o} = \overline{\rho}, \quad \frac{x}{c} = \overline{x},$$

and using the approximation for coefficient of viscosity, equation (13) appears in final form

$$\frac{dz}{d\overline{x}} + K\,(H+1)\,\frac{(d\overline{U}/d\overline{x})}{\overline{U}}\,z = K\,\overline{U}\,\frac{\overline{\rho} \times R_c}{[1 + 0.152\,M^2]} \qquad (15)$$

It is possible to put the solution of equation (15) in a form which is well adapted to calculations if constant average values are used for H and K. Under this assumption, the integral of the differential equation is

$$z = \overline{U}^{-K(H+1)} \left\{ C + \frac{R_c}{[1+0.152\,M^2]} \int K\,\overline{\rho}\,\overline{U}^{K(H+1)+1}\,d\overline{x} \right\} \qquad (16)$$

The variable ζ, in the turbulent region, lies roughly between 20 and 30 so that the total variation of K is small and K has an average value approximately equal to 1.21. The shape factor H varies, for a nonseparated boundary layer, approximately from 1.3 to about 1.7, but from experience gained in other calculations it has been found that computations for low speeds are quite insensitive to the value of H used and highly satisfactory results can be obtained for a constant value of H. In the present report K(H + 1) shall be set equal to 3. This assumes a value of H between 1.4 and 1.5 which is in conformity with low-speed measurements and, as shall be seen, will give computed drags in close agreement with experiment and other calculations. There are no available experimental measurements of velocity distributions through turbulent boundary layers at high speeds of sufficient accuracy to permit the determination of the effect of compressibility on H. Lacking such information, the assumption will be made that the same values for H can be used in the compressible case as in the incompressible case. Imposing the condition that at the transition point $z = z_{T.P.}$, the arbitrary constant C is determined and the solution becomes

$$z = z_{T.P.}\left(\frac{\overline{U}_{T.P.}}{\overline{U}}\right)^3 + \frac{1.21\,R_c}{[1+0.152\,M^2]\,\overline{U}^3} \int_{x_{T.P.}}^{x} \overline{\rho}\,\overline{U}^4\,d\overline{x} \qquad (17)$$

The density term in the integrand may be evaluated by assuming

the flow outside the boundary layer is isentropic; thus

$$\bar{\rho} = \left[1 + \frac{\gamma-1}{2} M^2 (1-\bar{U}^2)\right]^{\frac{1}{\gamma-1}} \tag{18}$$

The value of z at the transition point, which is required in equation (17), must be found from the value of $(\bar{\theta}\bar{\rho})_{T.P.}$ determined by equation (8). Since, in nondimensional variables,

$$\zeta = 2.555 \ln\left(\frac{4.075 R_c \bar{\theta} \bar{\rho} \bar{U}}{[1+0.152 M^2]}\right)$$

where ln denotes natural logarithms, then

$$z = 1.604 w \ln^2 w \tag{19}$$

if

$$w = \frac{4.075}{[1+0.152 M^2]} R_c \bar{\theta} \bar{\rho} \bar{U} \tag{20}$$

Substituting from equation (8) into equation (20) thus gives w at the transition point. In figure 2, which is a plot of equation (19), the required value of $z_{T.P.}$ can be found. If the velocity distribution over the airfoil and the free-stream Mach number are known it is now possible to substitute directly into equation (17) and determine the growth of the boundary layer up to the trailing edge.

Wake.- Young and Winterbottom in reference 10 have discussed the momentum equation in the wake and have concluded on the basis of what experimental data are available, that

$$\bar{\rho}_2 \bar{\theta}_2 = \bar{\rho}_{T.E.} \bar{\theta}_{T.E.} \bar{U}_{T.E.}^{3.2} \tag{21}$$

where subscript 2 applies at plane AA in the wake and T.E. indicates values at the trailing edge of the airfoil.

From $z_{T.E.}$ the value of $w_{T.E.}$ follows and the airfoil section profile drag coefficient is given by

$$c_d = [1+0.152 M^2] \frac{2 w_{T.E.}}{4.075 R_c} U_{T.E.}^{2.2} \tag{22}$$

Bodies of Revolution

Introductory remarks.— The development of the theory relating to the calculation of drag for a body of revolution is directly comparable to the theory presented above for airfoil sections except that the angle of attack of the body will be restricted to zero. In figure 3 the body is shown; point S representing the stagnation point, T.P. indicating the transition point in the plane of the paper, T.E. denoting the tail end of the body, and AA marking the position of the plane where static pressure has returned to its value in the ambient stream.

Drag coefficient of the body is by definition

$$C_D = \frac{D}{\frac{1}{2}\rho_o U_o^2 (V)^{2/3}} \tag{23}$$

where

D drag of body

U_o velocity in the free stream

ρ_o density in the free stream

V volume of body

and, from considerations of momentum,

$$D = 2\pi \int_w \rho u (U_o - u) y \, dy \tag{24}$$

where the integration extends across the wake in plane AA and

u local velocity in the wake

ρ density in the wake

y distance measured normal to center line of wake

For bodies of revolution the momentum area Φ which is defined by the equation

$$\Phi = 2\pi \int_o^\delta \frac{\rho u}{\rho_U U} \left(1 - \frac{u}{U}\right) (r + y \cos \alpha) dy \tag{25}$$

where

δ thickness of the boundary layer

r radius of cross section of body

α angle between tangent to generator and axis of body

occupies a role analogous to that of momentum thickness in two-dimensional airfoil theory. Momentum area in the wake, at the plane AA, is

$$\Phi_2 = 2\pi \int_w \frac{\rho u}{\rho_o U_o}\left(1 - \frac{u}{U_o}\right) y \, dy \tag{26}$$

whence

$$C_D = \frac{2\,\Phi_2}{(V)^{2/3}} \tag{27}$$

The theory which follows will also have occasion to use the variable θ which is related to the momentum area by the expression

$$\theta = \Phi/2\pi r \tag{28}$$

or

$$\theta = \int_o^\delta \frac{\rho u}{\rho_U U}\left(1 - \frac{u}{U}\right)\left(1 + \frac{y}{r}\cos\alpha\right) dy \tag{29}$$

Laminar layer.— From the theory developed in reference 11, the laminar boundary-layer thickness δ_1, defined as in the two-dimensional case, at an arbitrary point x_1 is given, neglecting terms involving the fourth power of M, by the expression

$$\left(\frac{d_1}{l}\right)^2 = \frac{1}{R_l\left(\frac{U_1}{U_o}\right)^{8.17}}\left(\frac{l}{r_1}\right)^2\left[5.3\left\{1-0.35\,M^2\left[1-1.91\left(\frac{U_1}{U_o}\right)^2\right]\right\}\right.$$

$$\left.\int_o^{\frac{x_1}{l}}\left(\frac{r}{l}\right)^2\left(\frac{U}{U_o}\right)^{8.17} d\left(\frac{x}{l}\right) - 0.44\,M^2\int_o^{\frac{x_1}{l}}\left(\frac{r}{l}\right)^2\left(\frac{U}{U_o}\right)^{10.17} d\left(\frac{x}{l}\right)\right] \tag{30a}$$

where

U_1 velocity outside boundary layer at point x_1

R_l Reynolds number based on length of body

r radius of cross section of body

x distance measured along axis

d_1 boundary-layer thickness as defined for equation (6a)

l axial length of body

Since, in general, the laminar portion of the boundary layer contributes a small part of the total drag and since the last term in equation (30a) represents a small part of the value given by the relation, it is practicable to derive a simplification for $(d_1/l)^2$ analogous to equation (6b). Thus,

$$\left(\frac{d_1}{l}\right)^2 = \frac{5.3}{R_l\left(\frac{U_1}{U_o}\right)^{8.17}}\left(\frac{l}{r_1}\right)^2\left\{1-0.35\,M^2\left[1-1.67\left(\frac{U_1}{U_o}\right)^2\right]\right\}$$

$$\int_o^{\frac{x_1}{l}}\left(\frac{r}{l}\right)^2\left(\frac{U}{U_o}\right)^{8.17}d\left(\frac{x}{l}\right) \qquad (30b)$$

It can also be shown that if Prandtl's number is set equal to 0.733 and if terms in M of fourth degree and higher are ignored, then for the body of revolution the following approximate relation is obtained

$$\left(\frac{\theta}{d}\frac{\rho U}{\rho_o}\right)^2_1 = 0.082\left\{1+0.61\,M^2\left[1-1.34\left(\frac{U_1}{U_o}\right)^2\right]\right\} \qquad (31)$$

Grouping momentum thickness and density together, and in nondimensional form, the following equation holds

$$\left(\frac{\theta}{c}\frac{\rho U}{\rho_o}\right)^2_1 = \frac{0.43}{R_l\left(\frac{U_1}{U_o}\right)^{8.17}}\left(\frac{l}{r_1}\right)^2\left\{1+0.26\,M^2\left[1-0.92\left(\frac{U_1}{U_o}\right)^2\right]\right\}$$

$$\int_o^{\frac{x_1}{l}}\left(\frac{r}{l}\right)^2\left(\frac{U}{U_o}\right)^{8.17}d\left(\frac{x}{l}\right) \qquad (32)$$

Turbulent layer.— The momentum equation of the boundary layer for a body of revolution in compressible flow is given in reference 12 in the form

$$\frac{\partial}{\partial x}\left(\rho_U U^2 \Phi\right) + \frac{\partial U}{\partial x}\left(\rho_U U \Delta^*\right) = \tau\, 2\pi r$$

where

Δ^* displacement area in boundary layer (see definition in list of symbols)

τ skin friction per unit of area

Setting $(\Delta^*/\Phi) = H$ reduces the equation for the boundary layer of the bodies of revolution to a form similar to that for airfoils. Thus

$$\frac{d\Phi}{dx} + \left[(H+2)\,\frac{U'}{U} + \frac{\rho' U}{\rho_U}\right]\Phi = \frac{\tau}{\rho_U U^2}\, 2\pi r \qquad (33)$$

the primes indicating differentiation with respect to x.

It should be noted that the definition of H differs in the three-dimensional case from that in two dimensions. However, in the case where the thickness of the boundary layer is small in comparison with the local radius of the body of revolution the two expressions for H are approximately equal.

The relation between τ, ρ, U, and θ used in the analysis for airfoil sections was based on theory that held for a flat plate; that is, the pressure gradients were ignored in that particular phase of the study. Since on bodies of revolution the pressure gradients are small, the same relation may be assumed to hold, thus

$$\frac{U\rho_U\theta}{\mu_w} = 0.2454 e^{0.3914\zeta} \qquad (34)$$

where

$$\zeta^2 = \frac{\rho_U U^2}{\tau}$$

From equation (34) and the definition of Φ, it follows that

$$\frac{U\rho_U\Phi}{\mu_w} = 0.2454\, 2\pi r\, e^{0.3914\zeta} \qquad (35)$$

and substitution of this relation into equation (33) gives

$$\frac{d\zeta}{dx} + 2.555\left[(H+1)\frac{U'}{U} + \frac{r'}{r}\right] = \frac{U\rho_U}{\mu_w} 10.411\zeta^{-2} e^{-0.3914\zeta} \tag{36}$$

Now let

$$z = \frac{U\rho_U}{\mu_w}\zeta^2 = 0.2454\zeta^2 e^{0.3914\zeta} \tag{37}$$

Direct substitution into equation (36) yields

$$\frac{dz}{d\left(\frac{x}{l}\right)} + K\left[(H+1)\frac{d(U/U_o)/d(x/l)}{U/U_o} + \frac{d(r/l)/d(x/l)}{r/l}\right] z = K\frac{U}{U_o}\frac{U_o\rho_o l}{\mu_w}\frac{\rho_U}{\rho_o} \tag{38}$$

where

$$2.555\left(0.3914 + \frac{2}{\zeta}\right) = K$$

and the equation is written in nondimensional form.

Setting

$$\frac{U}{U_o} = \overline{U},\ \frac{\rho_U}{\rho_o} = \overline{\rho},\ \frac{x}{l} = \overline{x},$$

and using the relation

$$\mu_w = \mu_o[1 + 0.152\ M^2]$$

the final form of equation (38) becomes

$$\frac{dz}{d\overline{x}} + K\left[(H+1)\frac{(d\overline{U}/d\overline{x})}{\overline{U}} + \frac{(d\overline{r}/d\overline{x})}{\overline{r}}\right] z = K\frac{\overline{U}\overline{\rho}R_l}{[1+0.152\ M^2]} \tag{39}$$

Putting again $K = 1.21$, $K(H+1) = 3$ and fixing the arbitrary constant of integration by assuming that $z = z_{T.P.}$ at $x = x_{T.P.}$, it is possible to express the solution of equation (39) in the form

$$z = z_{T.P.}\left(\frac{\bar{U}_{T.P.}}{\bar{U}}\right)^3\left(\frac{\bar{r}_{T.P.}}{\bar{r}}\right)^{1.21} + \frac{1.21\ R_l}{\bar{U}^3[1+0.152\ M^2]\bar{r}^{1.21}}\int_{x_{T.P.}}^{x} \bar{\rho}\ \bar{U}^4\ \bar{r}^{1.21}\ d\bar{x} \qquad (40)$$

The density term in the integrand is evaluated by means of the expression

$$\bar{\rho} = \left[1 + \frac{\gamma-1}{2} M_\infty^2(1 - \bar{U}^2)\right]^{\frac{1}{\gamma-1}} \qquad (41)$$

The determination of $z_{T.P.}$ from the known expression for $(\bar{\theta}\bar{\rho})$ given by equation (32), proceeds as follows: From equation (34)

$$\zeta = 2.555\ \ln\left(\frac{4.075\ R_l\ \bar{\theta}\ \bar{\rho}\ \bar{U}}{[1+0.152\ M^2]}\right)$$

whence

$$z = 1.604\ w\ \ln^2 w \qquad (42)$$

if

$$w = \frac{4.075\ R_l}{[1+0.152\ M^2]}\ \bar{\theta}\ \bar{\rho}\ \bar{U} \qquad (43)$$

Thus, from equations (43) and (32) the value of w at the transition point can be found and $z_{T.P.}$ is obtainable from figure 2. With this information, together with the velocity distribution over the body and the free-stream Mach number equation (40) can be used to trace the growth of the boundary layer aft of the transition point.

One difference arises in the computations for bodies of revolution which distinguishes the theory from that for airfoil sections. This is due to the fact that r vanishes at the tail of the body and as a consequence an infinite singularity appears in equation (40). Because of this singularity it is not possible to carry the integration to the tail for momentum thickness will become infinitely large and the expression for drag coefficient becomes an indeterminate form. To circumvent this difficulty it is necessary to use equation (40) up to some arbitrary point, say the 80-percent point

of the axis, and then to modify the method of calculation. For this purpose it is convenient to compute the growth of momentum area rather than momentum thickness over the latter portion of the turbulent run.

Two means will be given whereby the momentum area can be calculated. The first, which is merely an extension of reference 10 to the case of compressible flow, involves a point-by-point integration of the basic differential equation. This equation is expressible nondimensionally in the form

$$\frac{d\bar{\Phi}}{d\bar{x}} + \left[(H+2) \frac{\frac{d\bar{U}}{d\bar{x}}}{\bar{U}} \frac{\frac{d\bar{\rho}}{d\bar{x}}}{\bar{\rho}} \bar{\Phi} \right] = \frac{(0.3914)^2 \, 2\pi \bar{r}}{\ln^2 \dfrac{\bar{U} \, \bar{\rho} \, \bar{\Phi} \, R_l}{0.2454 \times 2\pi \bar{r} \times [1+0.152 \, M^2]}} \tag{44}$$

The derivation of this expression may be obtained by combining

$$\zeta^2 = \frac{\rho_U U^2}{\tau}$$

and

$$\frac{U \rho_U \Phi}{\mu_w} = 0.2454 \, 2\pi \, r \, e^{0.3914\zeta}$$

to get

$$\frac{\tau}{\rho_U U^2} = \frac{(0.3914)^2}{\ln^2 \dfrac{\bar{U} \, \bar{\rho} \, \bar{\Phi} \, R_l}{0.2454 \times 2\pi \bar{r} \times [1+0.152 \, M^2]}} \tag{45}$$

which, together with equation (33), will give the required relation.

From the value of $\bar{\theta}$ and $\bar{r}$ at the 80-percent point on the axis, the value of $\bar{\Phi}$ can be found at this point and the growth of $\bar{\Phi}$ can then be calculated over the remaining portion of the body. In particular, if $\bar{\Phi}_n$ is the value of $\bar{\Phi}$ at an arbitrary point $\bar{x}$ on the axis,

$$\bar{\Phi}_{n+1} = \bar{\Phi}_n + \left(\frac{d\bar{\Phi}}{d\bar{x}} \right)_n \Delta(\bar{x}) \tag{46}$$

where $\bar{\Phi}_{n+1}$ is the value of $\bar{\Phi}$ at the point $\bar{x} + \Delta(\bar{x})$. The calculation consists of repeated applications of this relation. As the interval $\Delta(\bar{x})$ in equation (46) gets smaller the result of

the calculation approaches the exact solution of equation (44).

Since the above calculation is to be applied over an interval which is small in comparison with the axial length of the body, the labor of such a calculation is much less than would be required if such methods were applied to the total turbulent run. It is possible, however, to shorten this calculation further by assuming that $c_f 2\pi \bar{r}$ is a linear function of $\bar{x}$ where $c_f = 2\tau/\rho_o U_o^2$ is the local skin-friction coefficient. The validity of such an assumption will be examined later in the discussion.

Return now to equation (33). From the definition of skin-friction coefficient the right-hand side of this equation is expressible as

$$\pi r \frac{2\tau}{\rho_o U_o^2} \frac{\rho_o}{\rho U} \left(\frac{U_o}{U}\right)^2 = \frac{2\pi r c_f}{2\rho U^2} \tag{47}$$

If $c_f 2\pi \bar{r}$ is linear over the aft portion of the body, falling from its value at the 80-percent point to zero at the tail, then in nondimensional terms equation (33) can be written as

$$\frac{d\bar{\Phi}}{d\bar{x}} + \left[(H+2)\frac{(d\bar{U}/d\bar{x})}{\bar{U}} + \frac{(d\bar{\rho}/d\bar{x})}{\bar{\rho}}\right]\bar{\Phi} = \frac{5}{2}(c_f 2\pi \bar{r})_{0.8} \frac{(1-\bar{x})}{\rho U^2} \tag{48}$$

This equation can be integrated, and as a result

$$\bar{\Phi} = \bar{U}^{-(H+2)} \bar{\rho}^{-1} \left[C + \int \frac{5}{2}(c_f 2\pi \bar{r})_{0.8} (1-\bar{x})\bar{U}^H \, d\bar{x}\right] \tag{49}$$

When $\bar{x} = 0.8$, $\bar{\Phi} = \bar{\Phi}_{0.8}$

so that

$$C = \bar{\Phi}_{0.8} \bar{U}_{0.8}^{H+2} \bar{\rho}_{0.8}$$

Using this value of C, together with equation (49),

$$\bar{\Phi} = \bar{\Phi}_{0.8}\left(\frac{\bar{U}_{0.8}}{\bar{U}}\right)^{H+2}\left(\frac{\bar{\rho}_{0.8}}{\bar{\rho}}\right) + \frac{5(c_f 2\pi \bar{r})_{0.8}}{2\bar{\rho}\bar{U}^{H+2}} \int_{0.8}^{\bar{x}} (1-\bar{x})\bar{U}^H d\bar{x} \tag{50}$$

and, after substituting from equation (47), the value of $\bar{\Phi}$ at the tail is given by the equation

$$\bar{\Phi}_{T.E.} = \bar{\Phi}_{0.8}\left(\frac{\bar{U}_{0.8}}{\bar{U}_{T.E.}}\right)^{3.5}\left(\frac{\bar{\rho}_{0.8}}{\bar{\rho}_{T.E.}}\right) + \frac{5}{6.528}\left[\frac{2\pi\,\bar{r}}{\ln^2\left(\frac{4.075\,R_l\,\bar{\theta}\,\bar{\rho}\,\bar{U}}{[1+0.152\,M^2]}\right)}\right]_{0.8}$$

$$\frac{\bar{\rho}_{0.8}\bar{U}_{0.8}^2}{\bar{\rho}_{T.E.}\bar{U}_{T.E.}^2}\int_{0.8}^{1.0}(1-\bar{x})\left(\frac{\bar{U}}{\bar{U}_{T.E.}}\right)^{1.5}d\bar{x} \qquad (51)$$

Wake.- In reference 12 Young has integrated the momentum equation in the wake applying the same methods used in references 2 and 10, for the body of revolution. If subscript 2 indicates values of the variables in the plane AA and T.E. denotes values at the tail of the body, then it is shown that

$$\bar{\rho}_2\,\bar{\Phi}_2 = \bar{\rho}_{T.E.}\,\bar{\Phi}_{T.E.}\,\bar{U}_{T.E.}^{3.2} \qquad (52)$$

Since, from equation (27)

$$C_D = \frac{2\Phi_2}{V^{2/3}}$$

it follows that

$$C_D = \frac{2\,\bar{\rho}_{T.E.}\,\bar{\Phi}_{T.E.}}{V^{2/3}\,l^2}\,\bar{U}_{T.E.}^{3.2} \qquad (53)$$

DISCUSSION

The foregoing theory provides a convenient procedure for studying the growth of laminar and turbulent boundary layers and for calculating the drag coefficients of airfoils and bodies of revolution. Just as in the case of wind-tunnel testing, where it is essential that the model tested be an accurate representation of the original configuration, it is important that in the application of this theory the operator should be able to determine correctly the required aerodynamic properties of the configuration under consideration. This implies that the pressure distribution over the body and the extent of the laminar and turbulent layers be specified or be determinable.

Velocity distributions are an immediate consequence of pressure distributions, for both low- and high-speed flow, so that if experimental data are available the calculations may proceed directly. The theoretical calculation of the velocity distribution corresponding to a given shape is, on the other hand, a rather lengthy process although such methods have been treated adequately in the literature. For an arbitrary airfoil section at any desired lift coefficient the velocity distribution for incompressible flow can be found by the methods of Theodorsen (reference 14), Allen (reference 15) or Goldstein (reference 16). For NACA conventional and low-drag airfoils corresponding distributions may be found quite easily from the tabular data given in reference 17. At subcritical Mach numbers the velocity distributions are calculable from low-speed data by means of the well-known Glauert-Prandtl or Karman-Tsien transformations. For the body of revolution, methods have been given by Young and Owen (reference 18) and Kaplan (reference 19).

The theory for the determination of velocity distributions is of course based on the assumption of potential flow but, for airfoils, if the lift coefficient rather than angle of attack is specified the calculations are sufficiently accurate for most applications. In reference 20 it is shown that the effect of the presence of a boundary layer is primarily to change the apparent angle of attack of the airfoil and to increase the local velocities in the vicinity of the trailing edge. A procedure is introduced in this reference for estimating the magnitude of the change in the trailing-edge velocity brought about by the presence of the boundary layer. This procedure first estimates boundary-layer thickness from the potential theory velocity distribution and can be used in conjunction with the theory of the present report. In the calculation of drag coefficient, however, the nature of the equation is such that the total drag coefficient computed is merely affected to a very small degree by moderate changes in the trailing-edge velocity, and as a consequence such a refinement is not used when only drag coefficient is to be found.

The determination of the location of the transition point from laminar to turbulent flow in the boundary layer presents a difficult problem. At small Reynolds numbers and for smooth surfaces transition occurs in a region of decreasing local velocities where there is usually a region of separated laminar flow between the laminar and turbulent portions of the boundary layer. However, at Reynolds numbers greater than several million the length of this region of separated laminar flow is of negligible extent so that it is possible to consider transition as occurring at a point. Experimental flight tests of smooth airfoils with maximum velocity in the vicinity of the midchord indicate that transition occurs when the local laminar boundary-layer Reynolds number $R_d = Ud\rho/\mu$ attains a value of about 8000. The velocity U is the local velocity outside the boundary layer and it should be noted in particular that the characteristic length d used in evaluating this Reynolds

number is the value of d obtained by the equation for the laminar boundary layer in the present report. This transition criterion applies strictly only to the determination of whether the transition point is ahead of the maximum velocity point. For configurations in which maximum velocity is as far back as the midchord position and for which the transition Reynolds number occurs aft of this point, it is probable that the transition point will be close behind the maximum velocity point. For smooth airfoils at angles of attack such that there is a sharp velocity peak in the vicinity of the leading edge, transition occurs behind the maximum velocity point. Theory and experiment indicate that in such cases transition at large Reynolds numbers occurs only after the velocity has decreased between 5 and 10 percent of the maximum velocity, the percentage of the velocity recovery before transition occurs being greater the more slowly the velocity decreases in the chordwise direction.

The preceding criteria for the location of the transition point indicate the most rearward position that can be expected, that is, the probable position for smooth airfoils in low-turbulence flow. When the surface under consideration is rough or contains such transition-promoting agents as protuberances, waves, air leakage, or dust particles ahead of the transition point, as predicted for ideal conditions, it is to be anticipated that transition will move forward in the direction of such disturbances. In the immediate vicinity of the stagnation point, however, there is a very rapid acceleration of the air so that any local disturbance which is not sufficiently severe to change the local velocity distribution will be unable to cause transition to occur in this region of very favorable velocity gradient.

There are not sufficient experimental data on the location of the transition point on bodies of revolution in low-turbulence flows. Lacking such information, the most reasonable basis for estimating the transition point on bodies of revolution seems to be to use the same criteria as previously presented for airfoils.

Drag of Airfoil Sections

In reference 2 the section drag coefficients, computed by the method of that report, are presented for an extensive range of airfoil thickness-chord ratios, Reynolds numbers, and transition point locations. A representative group of these cases has been recomputed by the methods of reference 4, as well as the present report, and the results of these calculations are given in table I. It is seen in the table that the maximum difference existing between the three methods for obtaining the drag coefficient is 0.0002 for a single surface and is 0.0004 for the total drag coefficient for both airfoil surfaces. There is no apparent consistency in the nature of the deviations, however, and in only one case does the

difference in total drag reach the value given above. The results of reference 4 should agree numerically with those of reference 2, since they are based on the same fundamental assumptions, but some difference might be expected when comparisons are made with the computations based on the present report because of the small change in the shape factor H and the averaging method used to fix the factor K. The agreement between the results should therefore be considered highly satisfactory and a confirmation of the compatibility of the assumptions.

The limits of accuracy of current methods for measuring airfoil section drag coefficients is of the same order of magnitude as the differences existing between the various theoretical results so that it is not possible to say which of the calculations most accurately predicts experimental values. The wake-survey method is now used commonly in the determination of experimental drag coefficient and it can certainly not be said to determine drag within the limits needed to establish the relative accuracy of the preceding computations even though, for a given test configuration, it may be possible to repeat measurements to a higher order of accuracy. Any experimental check is also complicated by the problem of locating the point of transition from the laminar to turbulent flow in the boundary layer. The previously mentioned methods for determining the transition point can easily err by a few percent of the chord length on each surface, and this can bring about an error in the calculated section drag coefficient of the order of magnitude of 0.0004.

Very few experiments have been conducted in which the location of transition from laminar to turbulent boundary-layer flow on both surfaces and the corresponding section drag coefficient were measured accurately. In reference 2 the section drag coefficient measured in flight is given as 0.0080 for a 25-percent-thick section at a lift coefficient of 0.25 and a Reynolds number of 8.2×10^6, the transition points having been measured and found to be 36 and 30 percent of the chord length, from the leading edge, on the upper and lower surfaces, respectively. For this configuration the following results are given by the various listed methods for calculating airfoil section drag coefficients:

Method	Section drag coefficient
Experimental, Flight (reference 2)	0.0080
Squire and Young (reference 2)	.0079
Nitzberg (reference 4)	.0077
Holt (reference 3)	.0076
Tetervin (reference 5)	.0077
Present report	.0080

These values are all within the probable limits of accuracy of experiment.

The drag coefficient for an NACA 0012 airfoil at zero angle of attack and the corresponding transition-point locations have been measured at a number of Reynolds numbers. These measurements are tabulated in reference 5 along with the theoretical drag coefficients obtained by several theoretical methods. The results, together with the numerical values calculated as indicated in the present report, are presented in table II. It is believed that the differences between the numerical values of the various methods leave little choice as to the relative accuracy. Any decision to use one method in preference to the others must rest, for the present, on convenience of application. The procedure of the present report requires no approximations to the velocity distribution over the airfoil and it is readily applied to calculating both the growth of the laminar and turbulent boundary layers as well as computing airfoil section drag coefficient.

The calculation of airfoil section drag coefficient for airfoils at speeds requiring the inclusion of compressibility effects was first given by Young and Winterbottom (reference 10). The single numerical example considered in this reference is an 18.5-percent-thick symmetrical Joukowski section at zero angle of attack. The assumption was made that the transition point is 9.4 percent of the chord from the leading edge and that the Reynolds number is equal to 10^7. Velocity distributions were used for potential flow and at a Mach number of 0.685. For these two cases the calculated drag coefficients were 0.0089 and 0.0091, respectively, while the present report gave, for the same data, the values 0.0089 and 0.0093. Thus, both methods indicate that at subcritical Mach numbers the introduction of compressibility effects into the computations brings about only a slight increase in the airfoil section drag coefficient.

Drag of Bodies of Revolution

The problem of boundary-layer growth and the determination of drag coefficient for bodies of revolution is more complex than for airfoil sections, since it is necessary to take into consideration the dimensions of the body as well as the velocity distribution. The method derived in the present report furnishes a procedure which parallels closely the analysis derived for an airfoil section and, with little increase in intricacy, embraces compressibility effects. In order to compare results obtained by the present method with results given in reference 12, drag coefficients of the Akron airship shape were computed at a variety of Reynolds numbers and transition points. These results are presented in table III along with the corresponding drag coefficients obtained by Young for the same configurations. (For convenience of comparison, Young's

convention of basing the drag coefficient on the body surface area was adopted. This convention differs from those used by the NACA which bases the drag coefficient on either the volume to the two-thirds power or on the projected frontal area.) It is noted that for transition points far forward the difference between the results for identical configurations, as obtained by the present method and that of Young, increases with the Reynolds number. This implies that the difference between the two methods arises in the calculation for the turbulent layer and is probably brought about by the use of the averaging method associated with the local skin-friction coefficient.

Very few experiments have been conducted on bodies of revolution at zero angle of attack to determine the location of transition and the corresponding drag coefficient. In reference 21 the drag-coefficient measurements for the Akron airship shape at three Reynolds numbers of the order of 10,000,000 are given. Boundary-layer surveys indicated that in each of these three cases the transition from laminar to turbulent boundary-layer flow occurred at 7 percent of the body length from the leading edge. In reference 22 drag coefficients are given at the same three Reynolds numbers for a metal body of virtually the same shape. These latter measurements are considerably larger, a fact which is difficult to explain because the pressure distribution over the forward 5 percent of the body is so very favorable that at these moderate test Reynolds numbers it is improbable that transition could move significantly ahead of the 7-percent station. For the series of measurements reference 22 indicates that the wind-tunnel-interference effect was of minor importance. The wooden model was of polygonal cross section; whereas the metal model was a true body of revolution but this would seem to be unimportant. Assuming that transition occurred at 7 percent of the body length from the leading edge and using the experimental pressure distribution of reference 21, the drag coefficient of the Akron shape was calculated at the three test Reynolds numbers.

In the following table the calculated values are compared with the two sets of experimental values.

Reynolds number	12.3×10^6	15.0×10^6	17.3×10^6
Wooden model	0.0198	0.0193	0.0190
Metal model	.0228	.0223	.0219
Theory	.0222	.0217	.0212

It is seen that the calculated values lie between the two sets of experimental data.

Raw data from wind-tunnel experiments on bodies of revolution generally indicate a change in the absolute value of the pressure coefficient as the Mach number increases but the magnitude of this increase is such that it may very well be attributable to wind-tunnel-wall effects. There is a difference of opinion between various authors as to the effects of compressibility on the velocity distribution over bodies of revolution for analyses have been presented both affirming and denying that pressure coefficients rise with increasing Mach numbers. These differences have been resolved by J. G. Herriot. In reference 23 he shows by means of linear perturbation theory that, for very slender streamline bodies of revolution in a uniform stream of compressible fluid, the pressure coefficient at the surface of the body is almost independent of Mach number. The equations of the present report, together with the result that the velocity distribution is independent of Mach number, were used to determine the effect of compressibility on the calculated drag coefficient for the Akron shape. For transition point at 25.7 percent of the chord from the leading edge, Reynolds number equal to 10^8, and free-stream Mach number equal to 0.7, this configuration had for calculated drag coefficient the value 0.00184 as compared with 0.00198 for the incompressible case.

In the presentation of the theory it was noted that the method developed for computing the growth of the boundary layer over bodies of revolution breaks down in the vicinity of the tail end. When the drag of the Akron shape was being computed it was observed that, over a range of Reynolds numbers from 10^6 to 10^8 and transition points from the leading edge to about the midchord position, in the step-by-step integration over the last 20 percent of the chord the quantity $c_f[2\pi(r/l)]$ varied almost linearly with x from its value at the 80-percent-chord station to zero at the trailing edge. In reference 12 this is also shown for Reynolds number equal to 10^8. When this assumption was inserted in the differential equation for Φ it was possible to integrate the equation directly and the results obtained by the direct integration were in good agreement with values obtained by the step-by-step integration of the original equation. It is believed that for practical applications the simplified procedure based on the assumption of a linear variation of $c_f[2\pi(r/l)]$ will be sufficiently precise. However, if a body of revolution, with shape markedly different over the rear portion from that of the Akron, is to be investigated for a range of transition points and Reynolds numbers it is suggested that representative cases be computed by using a step-by-step integration over the last 20 percent of the chord. Only in this manner can the exactness of the assumption concerning the linear variation of $c_f[2\pi(r/l)]$ be tested.

General Remarks

In certain cases it is particularly desirable to know the variation of either the thickness or the displacement thickness of the turbulent boundary layer over a curved surface or a body of revolution. In order to determine this precisely from a knowledge of the momentum thickness distribution it would be necessary, of course, to have added information about the variation of the shape factor H and the velocity distribution through the boundary layer. In reference 24, von Doenhoff and Tetervin have discussed certain aspects of this problem thoroughly, and have presented an empirical differential equation that, when used with the momentum equation and the skin-friction relation, permits tracing the development of the turbulent boundary layer to the separation point. The calculations necessary for the solution of these equations are, however, of considerable length.

The relations in reference 24 make it possible to calculate the variation of momentum thickness and boundary-layer-shape factor accurately. For airfoils at low speeds, this calculation involves the use of three equations:

$$\frac{d\theta}{dx} + (H+2)\frac{\theta}{U}\frac{dU}{dx} = \frac{1}{\zeta^2}$$

$$\zeta = 2.555 \ln (4.075 R_c \bar{\theta} \bar{U})$$

$$\theta \frac{dH}{dx} = e^{4.680 (H - 2.975)} \left[.2 \frac{\theta}{U}\frac{dU}{dx} \zeta^2 - 2.035(H-1.286) \right]$$

The first two of these equations are the basic equations of the present report and the last equation is an empirical relation which was developed by von Doenhoff and Tetervin. It so happens that the first equation is quite insensitive to the value of H. Thus for nonseparated flow the variation of θ, as computed by means of the method of the present report on the basis of the assumption of a constant value of H, is quite accurate. Once the chordwise distribution of θ is found the solution of the empirical equation of reference 24 is simplified considerably. If the numerical integration of the third equation above gives a value of H in excess of 1.8 at any chordwise station in the turbulent regime, the imminence of turbulent separation can be suspected and the method of the present report cannot be applied behind that station.

The present report treats the turbulent boundary layer in terms of the boundary-layer momentum thickness. Since, for an unseparated turbulent boundary layer a value of H, the ratio of displacement to

momentum thickness, of from 1.4 to 1.5 is indicated at low speeds and, since the effect of Mach number on H has been assumed to be negligible, the value of the displacement thickness follows immediately. In order to obtain the boundary-layer thickness, consistency demands the use of the type of velocity distribution which was used in the development of the logarithmic relation between the skin friction factor ζ and the boundary-layer momentum thickness. However, this approach involves theoretical difficulties which can be circumvented by the following means. It has been previously noted that the logarithmic relationship between the local skin-friction coefficient and the boundary-layer momentum thickness leads to a variation of local skin-friction coefficient with Reynolds number which is numerically equal to that predicted by the power law developed by Falkner in reference 7. This power law relationship between local skin friction coefficient and boundary-layer momentum thickness leads to the conclusion that the variation of velocity through the boundary layer is related to the distance normal to the surface by the expression

$$\frac{u}{U} = \left(\frac{y}{\delta}\right)^{1/5}$$

Using this approximation for the velocity profile it immediately follows the boundary-layer thickness is approximately $8.4\left(1 + \frac{M^2}{12}\right)$ times the boundary-layer momentum thickness.

In reference 4 and 20 it is shown, for a wide variety of airfoil sections, that the drag coefficients and boundary-layer-thickness distributions calculated from the Squire and Young equations agree well with experimental values. In the results that have been given in the present report, it has been shown that for various airfoil shapes and for a representative range of Reynolds numbers the calculated value of drag coefficient for each case is very close to that obtained by previously established methods, including those of Squire and Young. Since the method of the present report is of the same accuracy as previous methods and is more general and easily applied, its use in the calculation of drag coefficients and boundary-layer distributions is therefore recommended.

Ames Aeronautical Laboratory,
National Advisory Committee for Aeronautics
Moffett Field, Calif.

Max. A. Heaslet,
Physicist.

Gerald E. Nitzberg,
Aeronautical Engineer.

Approved:
Donald H. Wood,
Aeronautical Engineer.

APPENDIX A

Symbols

General Terms

c_f local skin-friction coefficient $(2\tau/\rho_o U_o^2)$

D drag of body (per unit length for airfoil section)

k thermal conductivity

M Mach number of free stream

Pr Prandtl's number $\left(\frac{c_p \mu}{k}\right)$

q_o dynamic pressure of free stream $(\frac{1}{2}\rho_o U_o^2)$

u local velocity inside boundary layer or in wake

U_o velocity of undisturbed stream

U local velocity outside boundary layer or at edge of wake

$\overline{U}$ nondimensional velocity ratio (U/U_o)

γ ratio of specific heats $[(c_p/c_v) = 1.4]$

δ boundary-layer thickness

ζ skin-friction factor $(\rho_u U^2/\tau)^{\frac{1}{2}}$

μ_o coefficient of viscosity in free stream

μ_w coefficient of viscosity at wall

ρ_o density in free stream

ρ_U density just outside boundary layer

ρ density inside boundary layer or wake

$\overline{\rho}$ nondimensional density ratio (ρ_U/ρ_o)

τ skin friction per unit area

Airfoil Sections

c airfoil chord

c_d section profile-drag coefficient $(D/\frac{1}{2}\rho_o U_o^2 c)$

H boundary-layer shape parameter (δ^*/θ)

R_c Reynolds number based on chord length $\left(\frac{\rho_o c U_o}{\mu_o}\right)$

w variable introduced in equation (19)

x distance along airfoil chord

$\bar{x}$ variable x in nondimensional terms (x/c)

y distance measured perpendicularly to airfoil surface or to center line of wake

$\bar{y}$ variable y in nondimensional terms (y/c)

z variable introduced in equation (12)

δ^* displacement thickness $\left[\int_o^\delta \left(1 - \frac{\rho u}{\rho_U U}\right) dy\right]$

θ momentum thickness $\left[\int_o^\delta \frac{\rho u}{\rho_U U}\left(1 - \frac{u}{U}\right) dy\right]$

$\bar{\theta}$ momentum thickness in nondimensional terms (θ/c)

Bodies of revolution

A surface area of body

C_A total drag coefficient $(D/\frac{1}{2}\rho_o U_o^2 A)$

C_D total drag coefficient $(D/\frac{1}{2}\rho_o U_o^2 V^{2/3})$

H boundary-layer parameter $\left(\frac{\Delta^*}{\Phi}\right)$

l length of body

r radius of cross section of body

$\bar{r}$ radius in nondimensional terms (r/l)

R_l Reynolds number based on length of body $\left(\frac{\rho_o l U_o}{\mu_o}\right)$

V volume of body

w variable introduced in equation (42)

x distance measured parallel to axis of body from stagnation point

$\bar{x}$ variable x in nondimensional terms (x/l)

y distance measured perpendicular to surface or to center line of wake

$\bar{y}$ distance y in nondimensional terms (y/l)

z variable introduced in equation (37)

α angle between tangent to generator and axis of body

Δ^* displacement area of boundary layer $\left[2\pi \int_o^\delta \left(1 - \frac{\rho u}{\rho_o U_o}\right)\left(r + y \cos \alpha\right) dy\right]$

displacement area of wake $\left[2\pi \int_o^\delta \left(1 - \frac{\rho u}{\rho_o U_o}\right) y \, dy\right]$

θ variable of integration $(\Phi/2\pi r)$

$\bar{\theta}$ nondimensional variable of integration (θ/l)

Φ momentum area of boundary layer $\left[2\pi \int_o^\delta \frac{\rho u}{\rho_o U_o}\left(1 - \frac{u}{U_o}\right)\left(r + y \cos \alpha\right) dy\right]$

momentum area of wake $\left[2\pi \int_o^\delta \frac{\rho u}{\rho_o U_o}\left(1 - \frac{u}{U_o}\right) y \, dy\right]$

$\bar{\Phi}$ momentum area in nondimensional terms $\left(\frac{\Phi}{l^2}\right)$

Subscripts

S conditions at stagnation point

T.E. conditions at trailing edge of airfoil or tail of body of revolution

T.P. conditions at transition point

w condition at wall or surface

o free-stream conditions

$\frac{1}{2}$	conditions in laminar boundary layer at arbitrary point x_1
0.8	conditions at 80-percent point on axis of body of revolution
2	conditions in wake where static pressure is that of free stream

APPENDIX B

Computation Procedure for Drag Calculation

1. Airfoil Section at Arbitrary Lift Coefficient

   A. From known airfoil thickness distribution or pressure distribution determine velocity distribution corresponding to desired lift coefficient.

   B. Estimate transition-point location on each surface by the following:

      (a) For maximum velocity in vicinity of leading edge, transition occurs at chordwise station corresponding to velocity decrease of from 5 to 10 percent of maximum velocity.

      (b) For maximum velocity in vicinity of mid-chord, transition occurs near maximum velocity point or, for large Reynolds numbers, ahead of maximum velocity point at chordwise station where local boundary-layer Reynolds number attains a value of about 8000.

$$R_\delta^2 = \frac{5.3\,R_c}{\bar{U}_{T.P.}^{7.17}}\left\{1 - 0.35\,M^2\left[1-1.67\,\bar{U}_{T.P.}^2\right]\right\}\int_0^{\bar{x}_{T.P.}} \bar{U}^{8.17}d\bar{x}$$

   C. From stagnation point to transition point the flow in boundary layer is laminar; thus at transition point

$$(\bar{\theta}\bar{\rho})_{T.P.}^2 = \frac{0.43}{R_c\,\bar{U}_{T.P.}^{9.17}}\left\{1 + 0.26\,M^2(1-0.92\,\bar{U}_{T.P.}^2)\right\}\int_0^{\bar{x}_{T.P.}} \bar{U}^{8.17}\,d\bar{x}$$

   D. Transform variable to $w_{T.P.} = \dfrac{4.075\,R_c}{1+0.152M^2}(\bar{\theta}\bar{\rho})_{T.P.}\bar{U}_{T.P.}$

   E. From figure 2 obtain $z_{T.P.} = 1.604\,w_{T.P.}\ln^2 w_{T.P.}$

   F. For turbulent region, from transition point to trailing edge, the growth of z is given by

$$z_{T.E.} = z_{T.P.}\left(\frac{\bar{U}_{T.P.}}{\bar{U}_{T.E.}}\right)^3 + \frac{1.21\,R_c}{[1+0.152M^2]\bar{U}_{T.E.}^3}\int_{\bar{x}_{T.P.}}^{\bar{x}_{T.E.}} \bar{\rho}\,\bar{U}^4\,d\bar{x}$$

where $\bar{\rho} = \left[1 + \frac{\gamma-1}{2} M^2 (1-\bar{U}^2)\right]^{\frac{1}{\gamma-1}} \approx [1+\frac{1}{2}M^2 (1-\bar{U}^2)]$

G. At trailing edge obtain $w_{T.E.}$ corresponding to $z_{T.E.}$ from figure 2.

H. Section drag coefficient is obtained from

$$c_d = \frac{2(1+0.152M^2)w_{T.E.}}{4.075\, R_c} \left(\bar{U}_{T.E.}\right)^{2.2}$$

2. Bodies of Revolution at Zero Angle of Attack

A. From body thickness distribution or pressure distribution determine velocity distribution.

B. Transition from laminar to turbulent flow occurs roughly at chordwise station where local boundary-layer Reynolds number attains a value of 8000.

$$R_\delta{}^2 = \frac{5.3\, R_l}{\bar{U}_{T.P.}{}^{7.17}} \frac{1}{\bar{r}_{T.P.}{}^2} \left\{1-0.35M^2\left[1-1.67\bar{U}_{T.P.}{}^2\right]\right\} \int_0^{\bar{x}_{T.P.}} \bar{r}^2 \bar{U}^{8.17} d\bar{x}$$

C. From stagnation point to transition point the flow in boundary layer is laminar; thus at transition point

$$(\bar{\theta}\,\bar{\rho})_{T.P.}{}^2 = \frac{0.43}{R_l \bar{U}_{T.P.}{}^{9.17} \bar{r}_{T.P.}{}^2} \left\{1 + 0.26\, M^2 \left(1-0.92\, \bar{U}_{T.P.}{}^2\right)\right\}$$

$$\int_0^{\bar{x}_{T.P.}} \bar{r}^2\, \bar{U}^{8.17} d\bar{x}$$

D. Transform variable to $w_{T.P.} = \frac{4.075 R_l}{1+0.152M^2} (\bar{\theta}\bar{c})_{T.P.} \bar{U}_{T.P.}$

E. From figure 2 obtain $z_{T.P.} = 1.604\, w_{T.P.} \ln^2 w_{T.P.}$

F. For turbulent region from transition point to 80-percent axial station, the growth of z is given by

$$z_{o.s} = z_{T.P.}\left(\frac{\bar{U}_{T.P.}}{\bar{U}_{o.s}}\right)^{3}\left(\frac{\bar{r}_{T.P.}}{\bar{r}_{o.s}}\right)^{1.21} + \frac{1.21\,R_l}{(1+0.152M^2)\bar{U}_{o.s}^{3}}$$

$$\int_{x_{T.P.}}^{\bar{x}_{o.s}} \frac{}{\bar{\rho}\bar{U}^4}\left(\frac{\bar{r}}{\bar{r}_{o.s}}\right)^{1.21} d\bar{x}$$

where $\bar{\rho} = \left[1 + \frac{\gamma-1}{2} M^2 (1-\bar{U}^2)\right]^{\frac{1}{\gamma-1}} \approx \left[1 + \frac{1}{2} M^2 (1-\bar{U}^2)\right]$

G. From figure 2 obtain $w_{o.s}$ corresponding to $z_{o.s}$

H. Transform variable to

$$\bar{\Phi}_{o.s} = 2\pi\,\bar{r}_{o.s}\,\bar{\theta}_{o.s} = \frac{2\pi\bar{r}_{o.s}w_{o.s}(1+0.152\,M^2)}{4.075\,R_l\bar{\rho}_{o.s}\bar{U}_{o.s}}$$

I. From 80-percent axial station to trailing edge, growth of $\bar{\Phi}$ is found from

$$\bar{\Phi}_{T.E.} = \bar{\Phi}_{o.s}\left(\frac{\bar{U}_{o.s}}{\bar{U}_{T.E.}}\right)^{3.5}\left(\frac{\bar{\rho}_{o.s}}{\bar{\rho}_{T.E.}}\right) + \frac{0.766(2\pi\bar{r}_{o.s})}{ln^2(w_{o.s})}\frac{\bar{\rho}_{o.s}\bar{U}_{o.s}^{2}}{\bar{\rho}_{T.E.}\bar{U}_{T.E.}^{2}}$$

$$\int_{o.s}^{T.E.} (1-\bar{x})\left(\frac{\bar{U}}{\bar{U}_{T.E.}}\right)^{1.5} d\bar{x}$$

J. The drag coefficient of the body of revolution, based on the volume to the two-thirds power, is then

$$C_D = \frac{2\rho_{T.E.}\bar{\Phi}_{T.E.}}{V^{2/3}l^2}\left(\bar{U}_{T.E.}\right)^{3.2}$$

REFERENCES

1. Prandtl, L.: The Mechanics of Viscous Fluids. Vol. III, div. G of Aerodynamic Theory, W. F. Durand, ed., Julius Springer (Berlin), 1935.

2. Squire, H. B., and Young, A. D.: The Calculation of the Profile Drag of Aerofoils. R. & M. No. 1838, British A.R.C., 1937.

3. Holt, Maurice: Calculation of Wing Profile Drag. Aircraft Engineering, vol. XV, no. 176, Oct. 1943, pp. 278–280.

4. Nitzberg, Gerald E.: A Concise Theoretical Method for Profile-Drag Calculation. NACA ACR No. 4B05, 1944.

5. Tetervin, Neal: A Method for the Rapid Estimation of Turbulent Boundary-Layer Thicknesses for Calculating Profile Drag. NACA ACR No. L4G14, 1944.

6. Kalikhman, L. E.: A New Method for Calculating the Turbulent Boundary Layer and Determining the Separation Point. Comptes Rendus de l'Academie des Sciences de l'URSS, 1943. Vol. XXXVIII, no. 5 to 6, pp. 165–169.

7. Falkner, V. M.: A New Law for Calculating Drag. The Resistance of a Smooth Flat Plate with Turbulent Boundary Layer. Aircraft Engineering, vol. XV, no. 169, Mar. 1943, pp. 65–69.

8. von Kármán, Th.: Turbulence and Skin Friction. Jour. Aero. Sci., vol. 1, no. 1, Jan. 1934, pp. 1–19.

9. Tetervin, Neal: Approximate Formulas for the Computation of Turbulent Boundary-Layer Momentum Thicknesses in Compressible Flows. NACA ACR No. L6A22, 1946.

10. Young, A. D., and Winterbottom, N. E.: Note on the Effect of Compressibility on the Profile Drag of Aerofoils in the Absence of Shock Waves. Rep. No. B.A. 1595, R.A.E. (British Confidential – U.S. Restricted), May 1940.

11. Allen, H. Julian, and Nitzberg, Gerald E.: The Effect of Compressibility on the Growth of the Laminar Boundary Layer on Low-Drag Wings and Bodies. NACA ACR, Jan. 1943.

12. Young, A.D.: The Calculation of the Total and Skin Friction Drags of Bodies of Revolution at Zero Incidence. R. & M. No. 1874, British A.R.C., 1939.

13. von Kármán, Th., and Tsien, H.S.: Boundary Layer in Compressible Fluids. Jour. Aero. Sci., vol. 5, no. 6, Apr. 1938, pp. 227-232.

14. Theodorsen, Theodore: Theory of Wing Sections of Arbitrary Shape. NACA Rep. No. 411, 1931.

15. Allen, H. Julian: General Theory of Airfoil Sections Having Arbitrary Shape or Pressure Distribution. NACA ACR No. 3G29, 1943.

16. Goldstein, S.: A Theory of Aerofoils of Small Thickness. Part I – Velocity Distributions for Symmetrical Aerofoils. Rep. No. 5804. Part II – Velocity Distributions for Cambered Aerofoils. Rep. No. 6156, A.R.C. (British Confidential – U.S. Restricted), 1942.

17. Abbott, Ira H., von Doenhoff, Albert E., and Stivers, Louis S., Jr.: Summary of Airfoil Data. NACA ACR No. L5C05, 1945.

18. Young, A.D., and Owen, P. R.: A Simplified Theory for Streamline Bodies of Revolution and its Application to the Development of High-Speed Shapes. Rep. No. Aero. 1837, R.A.E. (British Secret – U.S. Confidential), July 1943.

19. Kaplan, Carl: On a New Method for Calculating the Potential Flow Past a Body of Revolution. NACA ARR, July 1942.

20. Nitzberg, Gerald E.: The Theoretical Calculation of Airfoil Section Coefficients at Large Reynolds Numbers. NACA ACR No. 4I12, 1944.

21. Freeman, Hugh B.: Measurements of Flow in the Boundary Layer of a 1/40-Scale Model of the U.S. Airship "Akron." NACA Rep. No. 430, 1932.

22. Freeman, Hugh B.: Force Measurements on a 1/40-Scale Model of the U.S. Airship "Akron." NACA Rep. No. 432, 1932.

23. Herriot, John G.: The Linear Perturbation Theory of Axially Symmetric Compressible Flow, with Application to the Effect of Compressibility on the Pressure Coefficient at the Surface of a Body of Revolution. NACA (Proposed ACR).

24. von Doenhoff, Albert E., and Tetervin, Neal: Determination of General Relations for the Behavior of Turbulent Boundary Layers. NACA ACR No. 3G13, 1943.

TABLE I.- COMPARISON OF SECTION DRAG COEFFICIENT FOR SEPARATE AIRFOIL SURFACES COMPUTED BY VARIOUS METHODS

Thickness chord	Reynolds number	Upper surface x/c of T. P.	Lower surface x/c of T. P.	Section drag coefficient, cd					
				Reference 2		Reference 4		Present report	
				Upper surface	Lower surface	Upper surface	Lower surface	Upper surface	Lower surface
0	10^6	0	0	0.0046	0.0046	0.0046	0.0046	0.0047	0.0047
0	10^6	.2	.2	.0041	.0041	.0042	.0042	.0040	.0040
0	10^6	.4	.4	.0036	.0036	.0034	.0034	.0035	.0035
0	10^7	0	0	.0030	.0030	.0030	.0030	.0030	.0030
0	10^7	.2	.2	.0026	.0026	.0025	.0025	.0026	.0026
0	10^7	.4	.4	.0021	.0021	.0021	.0021	.0021	.0021
0	5×10^7	0	0	.0024	.0024	.0023	.0023	.0024	.0024
.14	10^6	.177	.177	.0065	.0050	.0063	.0050	.0063	.0049
.14	10^6	.376	.376	.0052	.0041	.0050	.0040	.0051	.0040
.14	10^7	.177	.177	.0041	.0031	.0040	.0031	.0041	.0031
.14	10^7	.376	.376	.0031	.0023	.0030	.0023	.0031	.0023
.25	10^6	.189	.196	.0091	.0066	.0091	.0065	.0089	.0064
.25	10^6	.386	.396	.0067	.0050	.0065	.0049	.0066	.0049
.25	10^7	.189	.196	.0057	.0041	.0060	.0041	.0059	.0042
.25	10^7	.386	.396	.0038	.0029	.0038	.0029	.0039	.0029

TABLE II.- COMPARISON OF EXPERIMENTAL DRAG COEFFICIENTS FOR NACA 0012 AIRFOIL SECTION AT ZERO ANGLE OF ATTACK WITH VALUES CALCULATED BY SEVERAL METHODS

Section drag coefficient, c_d					
Reynolds number $\times 10^{-6}$	Experimental measurement	Calculated reference 2	Calculated reference 3	Calculated reference 5	Calculated present report
2.675	0.0071	0.0074	0.0067	0.0069	0.0067
3.780	.0070	.0072	.0069	.0070	.0070
5.350	.0068	.0071	.0069	.0070	.0068
7.560	.0067	.0071	.0069	.0069	.0067

TABLE III.- THEORETICAL DRAG COEFFICIENTS OF AKRON AIRSHIP SHAPE CALCULATED AT SEVERAL REYNOLDS NUMBERS AND AT VARIOUS TRANSITION-POINT LOCATIONS

Reynolds number	Transition percent l	Drag coefficient, C_A	
		Present report	Reference 12
10^6	4.6	0.00502	0.00508
10^7	4.6	.00343	.00335
10^8	4.6	.00245	.00235
10^6	25.7	.00438	.00446
10^7	25.7	.00284	.00279
10^8	25.7	.00198	.00189
10^6	53.4	.00312	.00316
10^7	53.4	.00173	.00176
10^8	53.4	.00114	.00115

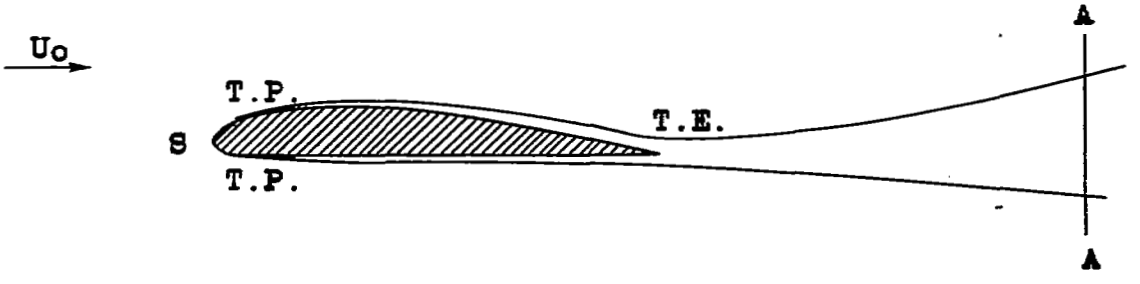

Figure 1.- Airfoil section with boundary layer.

NATIONAL ADVISORY COMMITTEE
FOR AERONAUTICS

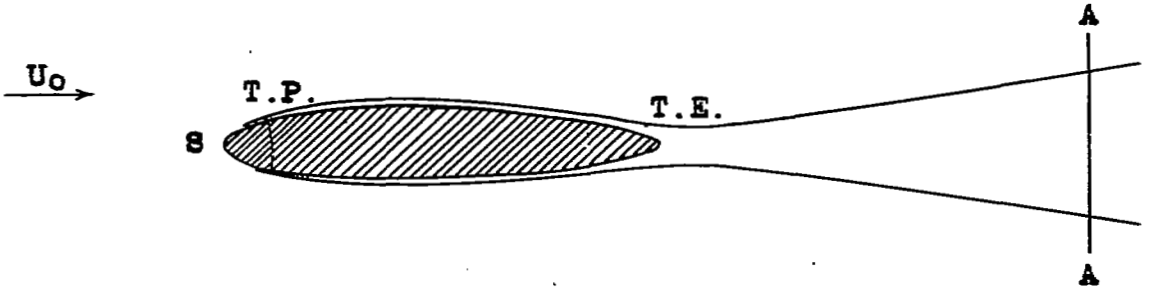

Figure 3.- Body of revolution with boundary layer.

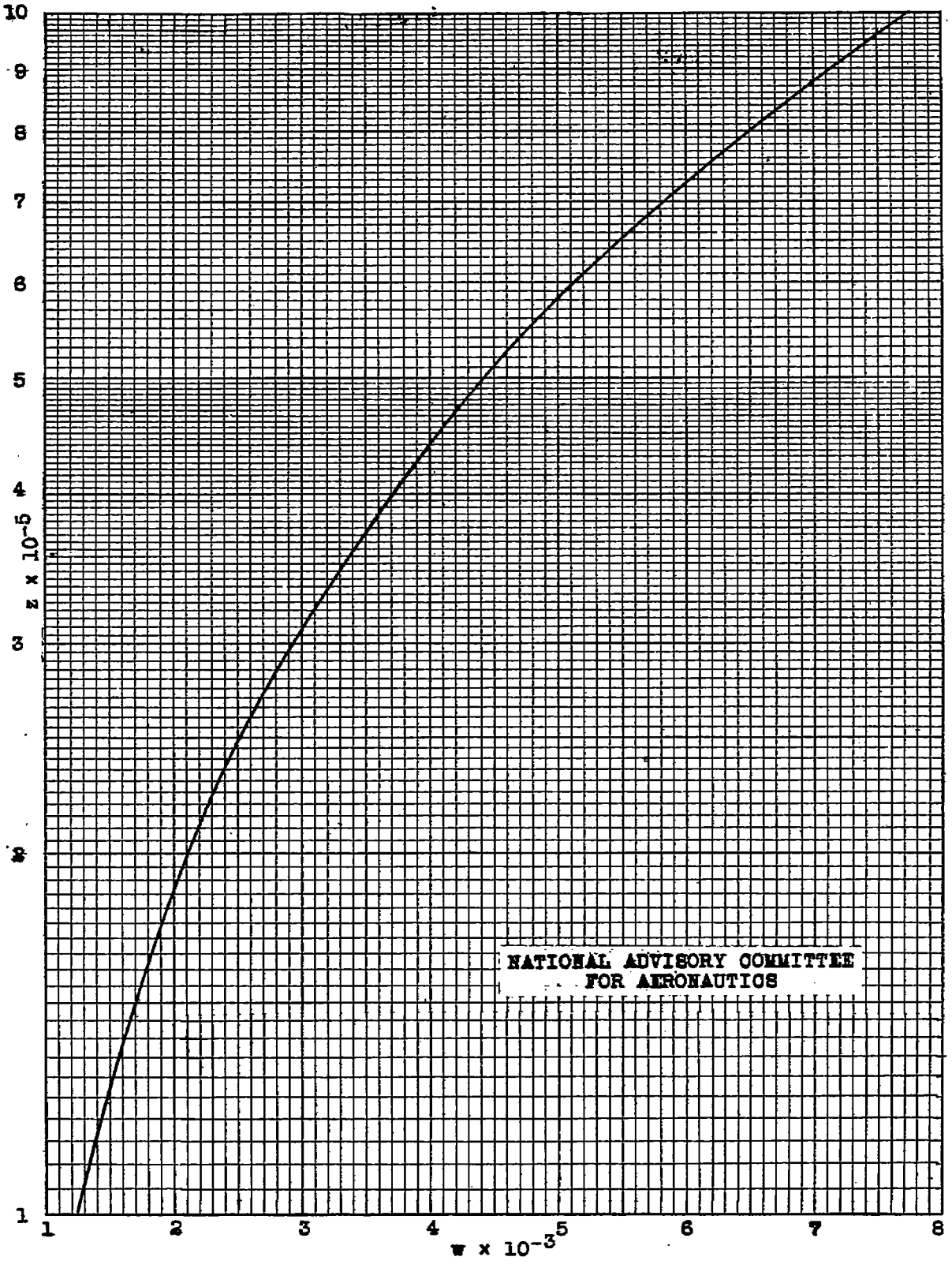

(a) Values of z from 10^5 to 10^6

Figure 2 (a to c).- Graph for evaluating w from z for turbulent boundary layers.

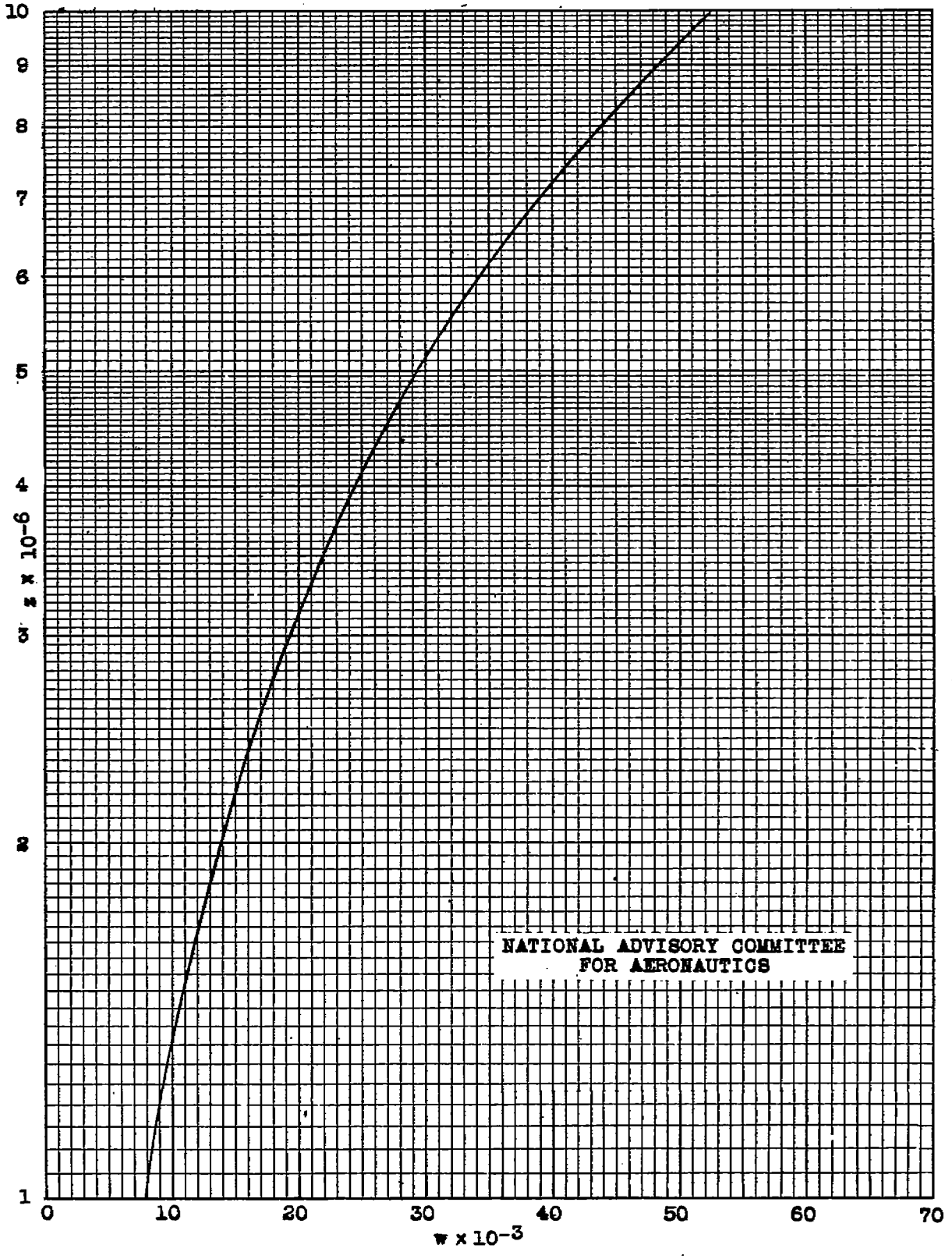

(b) Values of z from 10^6 to 10^7

Figure 2.- (Continued).

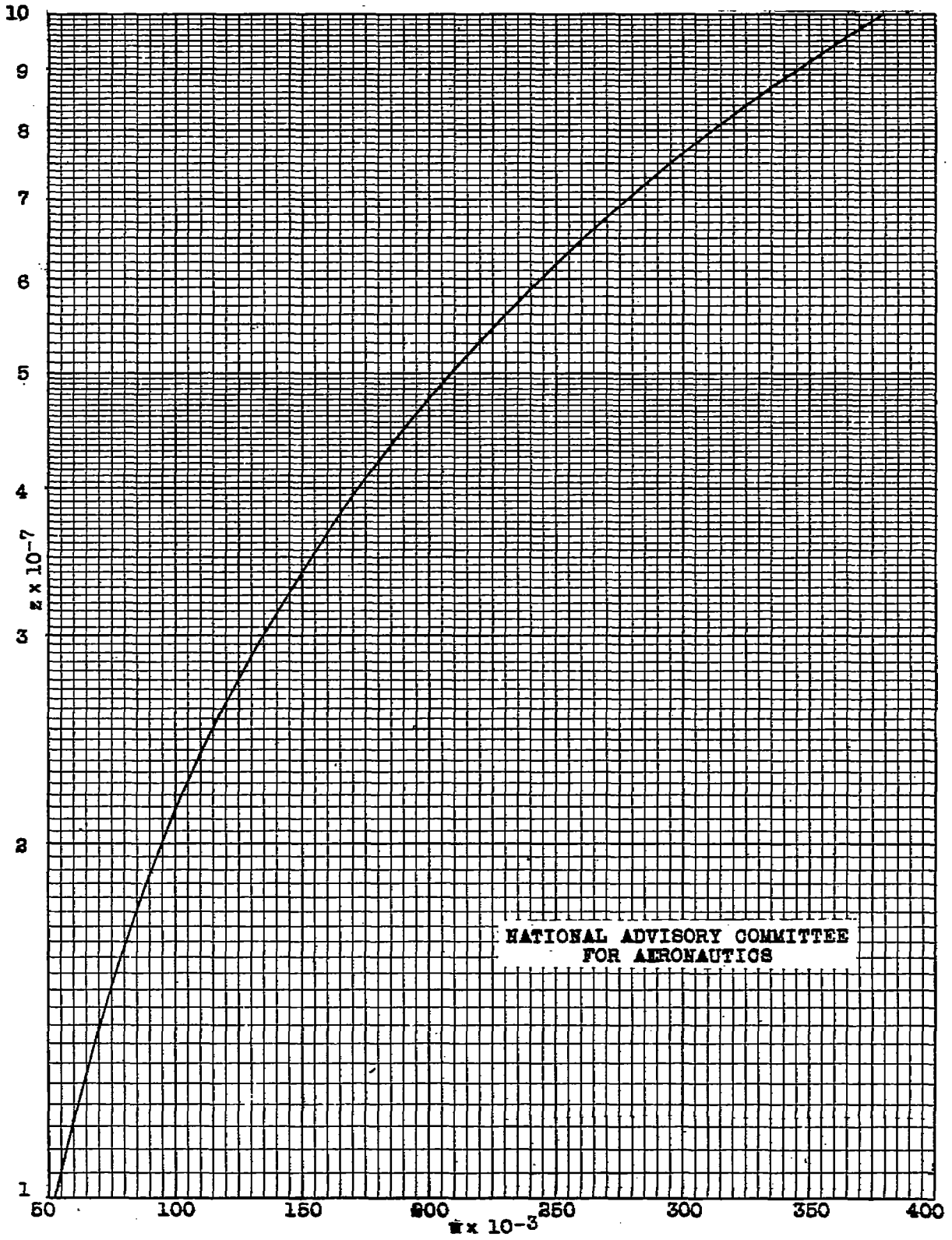

(c) Values of z from 10^7 to 10^8

Figure 2.- (Concluded).